Acta Cryst. (1997). **D53**, 658–664

Structure of Cytochrome *c*′ from *Rhodobacter capsulatus* Strain St Louis: an Unusual Molecular Association Induced by Bridging Zn Ions

TAHIR H. TAHIROV,[a]† SHINTARO MISAKI,[a] TERRY E. MEYER,[b] MICHAEL A. CUSANOVICH,[b] YOSHIKI HIGUCHI[a]‡ AND NORITAKE YASUOKA[a]*

[a]*Department of Life Science, Faculty of Science, Himeji Institute of Technology, Hyogo 678-12, Japan, and* [b]*Department of Biochemistry, University of Arizona, Tucson, AZ 85721, USA. E-mail: yasuoka@sci.himeji-tech.ac.jp*

(Received 26 August 1996; accepted 16 April 1997)

Abstract

Rhodobacter capsulatus strain St Louis cytochrome *c*′ (RCCP-SL) has been crystallized and the structure solved by molecular replacement. It was refined at 2.1 Å resolution to an *R* value of 18.4%, and compared with *Rhodobacter capsulatus* strain M110 cytochrome *c*′ (RCCP-M110). Although these two proteins are very similar in sequence and structure, the intermolecular interaction is largely different. In RCCP-M110, the molecules dimerize through interaction of helix *B* to form an antiparallel arrangement. When crystallized in the presence of Zn ions, molecules of RCCP-SL were found to be arranged as linear polymers connected by the bridging Zn ions. The changes in conformation of the side chains induced by binding of the Zn ions, by the substitution of Glu90 for Asp90, and by the different arrangement of the molecules, are discussed in detail.

1. Introduction

The *c*′ cytochromes comprise a unique class of heme proteins which function as electron carriers with intermediate oxidation–reduction potentials (0–150 mV) in the electron-transport chains of a wide variety of photosynthetic and denitrifying bacteria (Bartsch, 1978; Meyer & Kamen, 1982; Cusanovich, Meyer & Tollin, 1987). The three-dimensional structures of cytochromes *c*′ from *Rhodospirillum molischianum* (Weber *et al.*, 1980; Weber, Howard, Xuong & Salemme, 1981; Finzel, Weber, Hardman & Salemme, 1985), *Rhodospirillum rubrum* (Yasui *et al.*, 1992), *Chromatium vinosum* (Ren, Meyer & McRee, 1993), *Achromobacter xyloseoxidans* (formerly *Alcaligenes sp.*) and *Alcaligenes denitrificans* (Baker, Anderson, Dobbs & Dodson, 1995) have been reported.

Most cytochromes *c*′ are dimeric with each molecule comprising a left-handed four-α-helix bundle with a heme group attached to a Cys-*X*-*X*-Cys-His site near the carboxyl terminus. However, *Rhodobacter capsulatus* and *R. sphaeroides* cytochromes *c*′ appear to exist as equilibrium mixtures of monomers and dimers, and only *R. palustris* cytochrome *c*′ is completely monomeric (Cusanovich, 1971). In fact, the recently reported structures of strain M110 cytochrome *c*′ from *R. capsulatus* (RCCP-M110), which have been determined in two different crystal forms, show that the architecture of the RCCP-M110 dimer differs substantially from that of the other cytochromes *c*′ (Tahirov *et al.*, 1997). In the RCCP-M110 dimer, the molecules are roughly antiparallel to each other and only helix *B* of each molecule participates in the formation of the dimer interface. Furthermore, the dimer interface is smaller in RCCP-M110 than in the other reported cytochromes *c*′, where the molecules cross each other to form an X shape, and two helices, *A* and *B*, of each molecule interact across the dimer interface.

The cytochromes *c*′ can be divided into two groups based upon heme accessibility (Tahirov *et al.*, 1997). The group 1 cytochromes *c*′, including RCCP, have a deep channel between helices *B* and *C* with direct solvent access to the heme sixth ligand position, whereas there is no such channel in group 2 cytochromes *c*′. Group 1 cytochromes *c*′ can bind larger heme ligands, such as alkylisocyanides, with high affinity (Rubinov & Kassner, 1984; Patel, Kassner, Meyer & Cusanovich, 1989; Kassner, 1991). Some of the group 1 cytochromes *c*′, for example from *Chromatium vinosum*, undergo dimer–monomer dissociation upon binding heme ligands (Doyle, Gill & Cusanovich, 1986). The structure of *n*-butylisocyanide-bound RCCP-M110 shows that ligand binding induces an unusual concerted movement of side chains in the heme vicinity, which may cause dimer dissociation in some species, such as *C. vinosum* (Tahirov *et al.*, 1996).

The primary structure of cytochrome *c*′ from *R. capsulatus* strain St Louis (RCCP-SL) shows 11 substitutions in the amino-acid sequence compared with strain SP7, which is closely related to the type strain, ATH2.3.1 (Ambler *et al.*, 1981; Ambler, personal communication). The RCCP-M110 used for the previous

† Present address: Institute for Protein Research, Osaka University, Yamadaoka 3-2, Suita, Osaka 565, Japan. Permanent address: Institute of Inorganic and Physical Chemistry, Azerbaijan Academy of Sciences, Javid Avenue 29, Baku 370143, Azerbaijan.

‡ Present address: Division of Chemistry, Graduate School of Chemistry, Kyoto University, Sakyo-ku, Kyoto 606, Japan.

© 1997 International Union of Crystallography
Printed in Great Britain – all rights reserved

ISSN 0907-4449 ©1997

structure determination (Tahirov *et al.*, 1997) appears to differ from RCCP-SL used here in one residue only. The Asp90 in RCCP-SL is substituted for Glu90 in RCCP-M110. In the current report, we present the crystallization, three-dimensional structure determination and the refined crystal structure of RCCP-SL, in which the molecular interaction differs markedly from that of RCCP-M110.

2. Experimental

2.1. *Crystallization and data collection*

Macromolecular crystallization reagent kits, 'Crystal Screen' and 'Crystal Screen II', purchased from Hampton Research, were used for screening crystallization conditions. The procedure was the same as that suggested by Jancarik & Kim (1991). RCCP-SL crystals were grown in 3 d as extremely thin parallelepiped plates, with dimensions 0.6 × 0.25 × 0.004 mm, by the sitting-drop vapor-diffusion method. Drops were composed of a mixture of 5 µl of 10 mg ml^{-1} protein solution and 5 µl of a reservoir solution; they were equilibrated against 500 µl of reservoir solution at room temperature. The reservoir solution was prepared by mixing equal amounts of 18% PEG 8000 as precipitant, 0.2 *M* zinc acetate as salt and 0.1 *M* sodium cacodylate buffer at pH 6.5. These conditions were derived considering the fact that RCCP-SL does not crystallize under the same conditions as RCCP-M110 (Higuchi *et al.*, 1996; Tahirov *et al.*, 1997). Furthermore, RCCP-M110 does not crystallize under the conditions reported here for crystallization of RCCP-SL. The RCCP-SL crystals belong to the monoclinic space group $P2_1$, with unit-cell dimensions $a = 39.68$, $b = 46.85$, $c = 40.75$ Å, $\beta = 110.94°$. The solvent content calculated using the Matthews (1968) equation suggests that there are two 14 kDa molecules in the unit cell with an approximate water content of 51%.

Diffraction patterns were recorded on Fuji imaging plates with a Weissenberg camera for protein crystallography installed on BL-6A at the Photon Factory of the National Laboratory for High Energy Physics in Tsukuba (Sakabe, 1991). The wavelength of the synchrotron radiation source was 1.0 Å. Crystals diffracted to at least 2.1 Å resolution and only one crystal was used to collect the complete data set. The recorded data were read by a BA-100 system and processed with the programs *DENZO* and *SCALEPACK* (Otwinowski, 1986). A total of 27 125 reflections in the resolution range 30–2.1 Å were merged to give 6988 independent intensities with an $R_{\rm merge}$ value of 0.08, data completeness of 85.2% and $\langle I/\sigma(I)\rangle = 16.0$. The last three values were 0.19, 66.4% and 3.9, respectively, in the last resolution shell from 2.18 to 2.1 Å.

2.2. *Structure solution and refinement*

The atomic coordinates of crystal form *A* of RCCP-M110 (accession number 1CPQ in the Brookhaven Protein Data Bank) were used as a search model (Tahirov *et al.*, 1997). The molecular replacement method based on Patterson correlation (PC) refinement (Brünger, 1990*a*) gave a clear solution in the resolution range 15–4 Å, with a PC coefficient of 0.39 for the first peak of the cross-rotation function; the PC coefficient for the highest background peak was 0.15. The best solution corresponds to a set of rotation angles $\theta_1 = 177.4$, $\theta_2 = 98$ and $\theta_3 = 263.8°$. The translation search for the same resolution data also gave a clear solution with the fractional coordinates at $x = 0.275$, $y = 0$, $z = 0.561$, and a correlation coefficient of 0.62 (0.48 for the next peak and a value of $\sigma = 0.04$). Structure refinements by rigid-body, conjugate-gradient minimization, simulated-annealing and *B*-factor refinement protocols of the *X-PLOR* program package (Brünger, 1990*b*), with the parameters set at parhcsdx.pro (Engh & Huber, 1991), reduced the crystallographic *R* factor from 39.8 to 23.2% in the resolution range 6.0–2.1 Å. $(2F_o - F_c)$ and $(F_o - F_c)$ Fourier maps and omit maps clearly indicated the substitution of Glu90 (in RCCP-M110) for Asp90, as

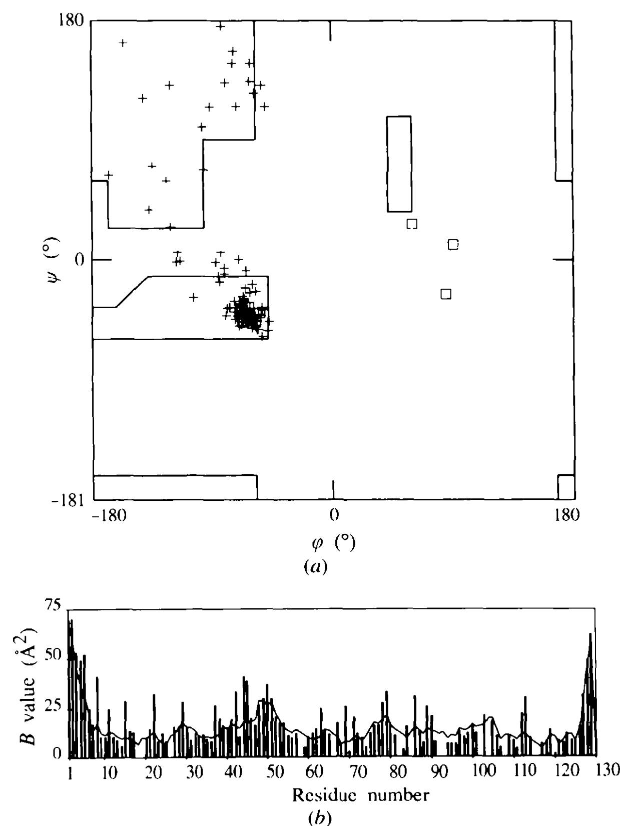

Fig. 1. The quality of the refined model of RCCP-SL. (*a*) Ramachandran plot. The glycine residues are shown as squares. (*b*) Plot of the average *B* values (Å^2). The average *B* values for the main-chain atoms are indicated by a continuous line and the average *B* values for the side-chain atoms are shown by vertical bars. The average *B* value for the heme is shown at position 130.

expected from the primary structure of RCCP-SL (Ambler, personal communication). At this stage, 47 water molecules were located. An additional six peaks had unacceptable protein–water distances of approximately 2.05 Å and high density values on the electron-density maps. Two of them, especially, had values comparable to that of Fe. These six peaks, in addition to a peak for heme Fe, appeared in the anomalous difference Fourier map calculated from 4911 Friedel pairs at 2.2 Å resolution, with phases obtained from the coordinates of the refined molecule, indicating the presence of heavy atoms at these positions rather than water. Considering the crystallization reagents, two types of heavy atom are possible: Zn or As. The binding geometry suggests the presence of Zn ions. The positions and the occupancies of the Zn ions were also refined. Finally, the overall and individual displacement parameters were refined again. The final crystallographic R value for 962 protein atoms, six Zn atoms and 47 water O atoms was 18.4% for 6440 reflections with $F \geq 2\sigma(F)$ in the resolution shell from 6 to 2.1 Å, which corresponds to 81.5% of all possible reflections. The resulting root-mean-square (r.m.s.) deviations from standard values for bond lengths, bond angles, dihedral angles and improper angles are 0.009 Å, 1.34, 20.02 and 1.51°, respectively. The r.m.s. B values for protein atoms, Zn ions and water O atoms are 21.1, 23.6 and 36.0 Å^2, respectively. A Ramachandran plot and a plot of displacement parameter *versus* residue number are shown in Fig. 1. The atomic coordinates of the refined structure have been deposited in the Brookhaven Protein Data Bank (Bernstein *et al.*, 1977; Abola, Bernstein, Bryant, Koetzle & Weng, 1987).†

3. Results and discussion

RCCP-M110 was crystallized in two different crystal forms, *A* and *B*. In both forms, the molecules appear to be dimers and their dimer structures are very similar to each other (Tahirov *et al.*, 1997). However, RCCP appears to exist as an equilibrium mixture of monomers and dimers in solution (Cusanovich, 1971). Although a comparison of RCCP-M110 and RCCP-SL shows only a single amino acid substitution and that their molecular folds (Fig. 2*a*) are identical, the association of molecules in the current crystal form of RCCP-SL is totally different from that in RCCP-M110. RCCP-SL crystallized as a linear association of monomers, extended along the *c* axis (Fig. 2*b*), rather than as dimers. There are some intermolecular salt bridges, water-mediated hydrogen bonds and hydrophobic contacts in the crystal that are different from those in the RCCP-M110 structure (Table 1). However, we believe that the change in architecture is caused by the presence of Zn ions, as described below.

Table 1. *Intermolecular contacts in RCCP-SL*

Hydrogen bonds	Hydrophobic interactions
Asn77 ND2^{i}···Glu34 O^{ii}	Pro53 CA^{i}···Ala97 CB^{iii}
Asn77 ND2^{i}···H_2O 24^{i}···Glu34 O^{ii}	Pro53 CB^{i}···Ala97 CB^{iii}
Asn100 ND2^{i}···H_2O 27^{i}···Ala1 N^{iii}	Pro53 CG^{i}···Ala94 CA^{iii}
Glu11 OE2^{i}···Lys119 NZ^{iv}	Pro65 CG^{i}···Leu111 CD2^{iv}
S61 O^{i}···Gln112 NE2^{iv}	Pro65 CD^{i}···Thr25 CG2^{iv}
Thr68 O^{i}···H_2O 41^{i}···Gly66 N^{iv}	Gly66 CA^{i}···Gly115 CA^{iv}
Thr68 O^{i}···H_2O 41^{i}···Gln112 OE1^{iv}	Gly66 CA^{i}···Gly116 CA^{iv}
	Ala76 CB^{i}···Val38 CG2^{ii}

Symmetry codes: (i) x, y, z; (ii) $x, y, z-1$; (iii) $-x, 0.5+y, -z$; (iv) $1-x, 0.5+y, -z$; (v) $x, y, z+1$; (vi) $-x, -0.5+y, -z$; (vii) $1-x, -0.5+y, -z$. The symmetry-related mate for (i)–(ii) is (v)–(i), for (i)–(iii) is (vi)–(i), and for (i)–(iv) is (vii)–(i).

The overall structures of RCCP-M110 and RCCP-SL molecules are similar; they can be superimposed at the Cα positions of 129 residues and at the heme Fe-atom positions with an r.m.s. deviation of 0.39 Å. The deviation of Cα positions *versus* residue number is plotted in Fig. 3. The difference between RCCP-M110 and RCCP-SL is larger at the N- and C-terminal ends. This is not unexpected, since the *B*-value distributions in RCCP-SL (Fig. 1*b*), as well as in two crystal forms of RCCP-M110 (Tahirov *et al.*, 1997) and in *n*-butylisocyanide-bound RCCP-M110 (Tahirov *et al.*, 1997), indicate that their terminal regions are highly flexible or disordered.

The only difference in primary structure between RCCP-M110 and RCCP-SL is at position 90. In RCCP-M110, Glu90 is far from the dimer interface and, consequently, it is inappropriate to expect that the substitution of Glu90 for Asp90 in RCCP-SL changes the dimer architecture or drives dimer dissociation. However, such a substitution seems to influence dramatically the crystallization process. Crystals of RCCP-SL do not grow under the conditions used for crystallization of the two polymorphs of RCCP-M110. Comparison of the RCCP-M110 and RCCP-SL structures (Fig. 4) shows that the Glu90 to Asp90 substitution affects only the position of the adjacent side chain, Lys86. In RCCP-M110, the position of the Lys86 side chain is stabilized by a salt bridge between Lys86 NZ and Glu90 OE1. In addition, a weaker salt bridge is formed between Lys86 NZ and Glu5 OE2 of the neighboring molecule (Fig. 4). The RCCP-SL structure shows that both salt bridges are disrupted by the Glu90 to Asp90 substitution, and both seem essential for stabilizing the crystal structure of RCCP-M110. In addition to the fact that crystals of RCCP-SL do not grow under the conditions used for crystallization of two polymorphs of RCCP-M110 (as mentioned above), crystals of RCCP-M110 do not grow under the conditions used for crystallization of RCCP-SL. However, inspection of the crystal structure of RCCP-SL shows that the space

† Atomic coordinates and structure factors have been deposited with the Protein Data Bank, Brookhaven National Laboratory (Reference: 1CPR and R1CPRSF). Free copies may be obtained through The Managing Editor, International Union of Crystallography, 5 Abbey Square, Chester CH1 2HU, England (Reference: TS0003).

around the Asp90 and Lys86 side chains is large enough to accommodate the Asp90 to Glu90 substitution and the associated conformational changes of the Lys86 side chain without detectable influence on the surrounding molecules. One possibility why the crystals of RCCP-M110 do not grow under the conditions used for crystallization of RCCP-SL is that the Glu90 side chain might bind Zn ions. The results also suggest that the dimer observed in RCCP-M110 is stabilized by crystal packing and may not be the same as the dimer that is present in solution. Thus, the forthcoming results of an NMR study of the structure in solution should be informative (Caffrey, Simorre, Brutscher, Cusanovich & Marion, 1995).

The six peaks on electron-density maps were assigned to Zn ions. The overall locations relative to the RCCP-SL molecule are shown in Fig. 2. The configuration about Zn1 is tetrahedral (Fig. 5). This position is fully occupied and the Zn is located between two molecules related by a translation along the *c* axis. Zn1 binds to both molecules, to OD2 of Asp32 and OE1 of Glu34 from one molecule, and to OD2 of Asp124 from another molecule. The average Zn—O distance is 2.05 Å. The distance to the fourth coordination position, occupied by heavy atom 2, is 3.17 Å. We assigned this heavy atom to Zn with an occupancy of 0.35. However, a disordered cacodylate ion at the Zn2 position cannot be ruled out. Zn4 has an occupancy 0.45 and binds to O2A of the heme propionate and OE2 of Glu11 with a Zn—O distance of 2.06 Å. The binding of Zn4 results in breakage of a salt bridge between NZ of Lys15 and O1A of the heme propionate and in reorientation of the Glu11 side chain as

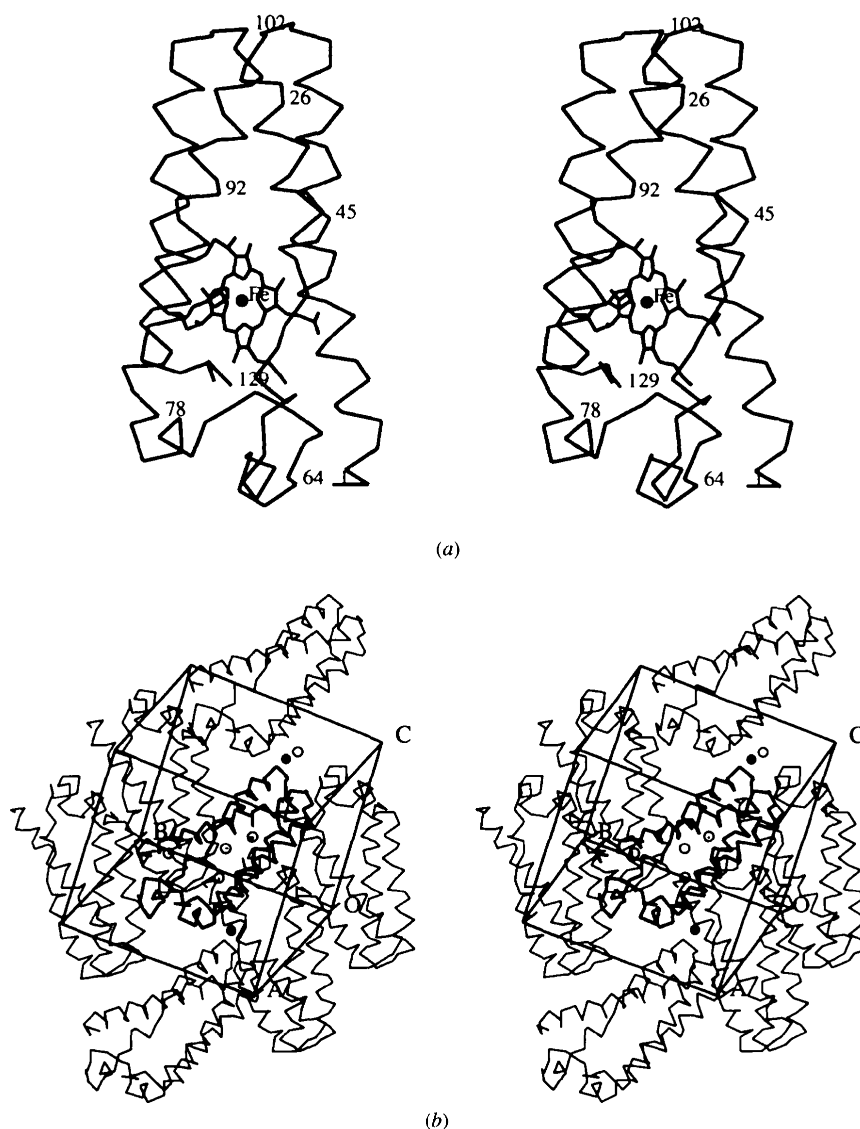

Fig. 2. Molecular and crystal structure of RCCP-SL. (*a*) Cα backbone of RCCP-SL molecule with an attached heme group. (*b*) Crystal packing in RCCP-SL showing the two bridging Zn1 atoms, which connect molecules translated along the *c* axis. A single molecule (thick lines) is surrounded by six nearest-neighbour molecules (thin lines). Zn1 atoms are drawn as solid spheres and the other five Zn atoms as open spheres.

compared with the RCCP-M110 structure (Fig. 6). The three remaining Zn ions are bound to imidazole N atoms, Zn3 to ND1 of the heme ligand His122, Zn5 to ND1 of His89, and Zn6 to NE2 of His89, with an average Zn—N distance of 2.11 Å. The occupancy of Zn3 is 0.7 and is higher than the occupancies of Zn5 and Zn6, which are 0.31 and 0.25, respectively. In RCCP-M110, the His89 side chain is disordered and occupies two positions. However, no disorder was observed for His89 in RCCP-SL.

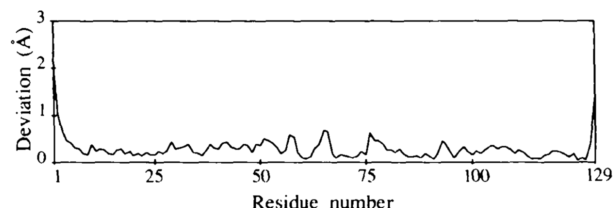

Fig. 3. The deviation of $C\alpha$ positions (Å) in RCCP-M110 relative to their positions in RCCP-SL *versus* residue number.

Only a few interactions across the dimer interface were observed in the RCCP-M110 structure. These include a hydrophobic interaction between Val38 and Ile46, two salt bridges between the side chains of Glu39 and Lys42, and between Glu34 and Thr49, and their symmetry-related pairs, plus some water-mediated hydrogen bonds. In RCCP-SL, the side chain of Glu34 binds a Zn ion (Zn1) and changes conformation relative to that in RCCP-M110, thus leading to breakage of the hydrogen bond across what would have been the dimer interface.

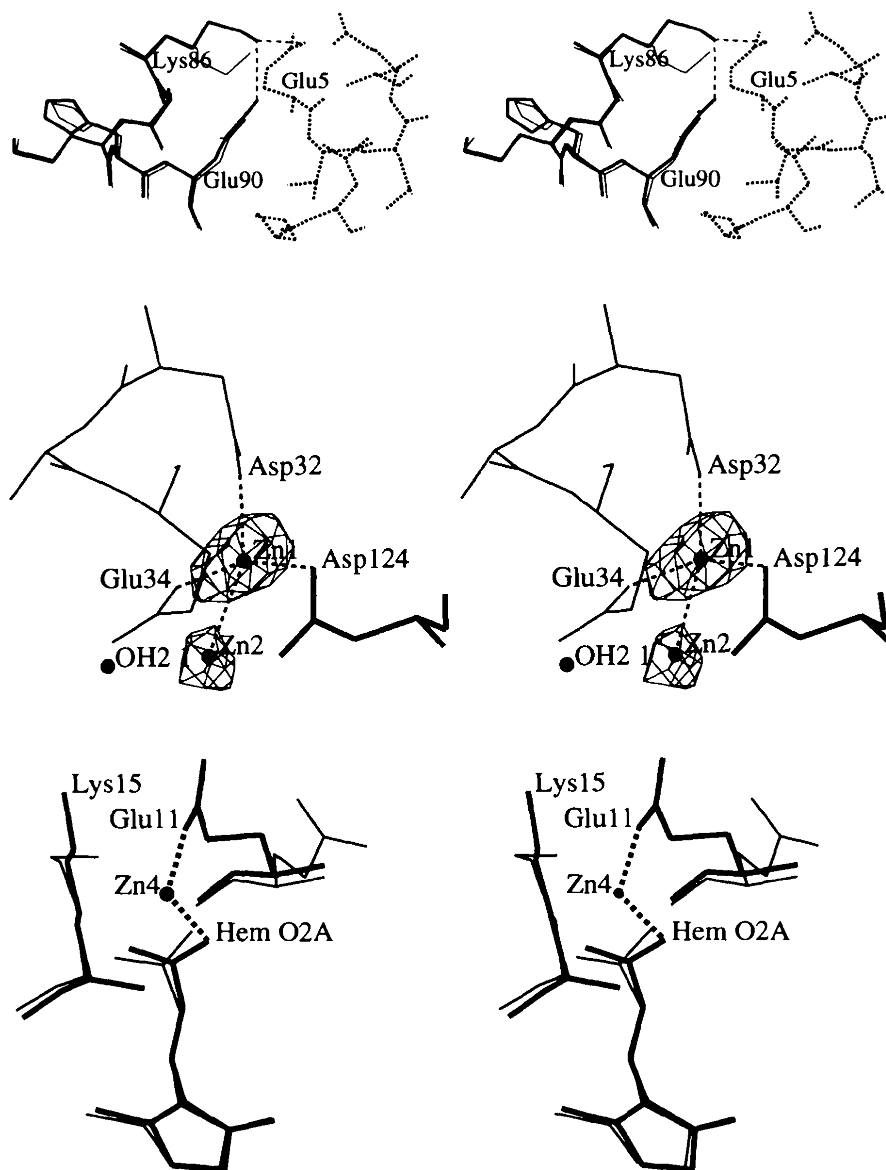

Fig. 4. Comparison of side chains in positions 86 and 90 in RCCP-SL with those of RCCP-M110 crystal form *A*. The RCCP-M110 molecule is represented by thick lines and the superimposed RCCP-SL molecule is represented by thin lines. The neighboring RCCP-M110 molecule (thick dashed lines) and hydrogen bonds from Lys86 to Glu5 and Glu90 (thin dashed lines) are also shown.

Fig. 5. The coordination of Zn1 and Zn2 ions. The Asp32 and Glu34 residues are of one molecule (thin lines), and Asp124 is of the molecule related by symmetry $(x, y, z+1)$ (thick lines). The coordination of Zn is represented by dashed lines. The anomalous Fourier map, covering the Zn ions, is contoured at 5σ.

Fig. 6. The conformational changes induced by binding of Zn4. RCCP-M110 is draw with thin lines, RCCP-Sl is drawn with thick lines, and the Zn coordination is shown by dashed lines.

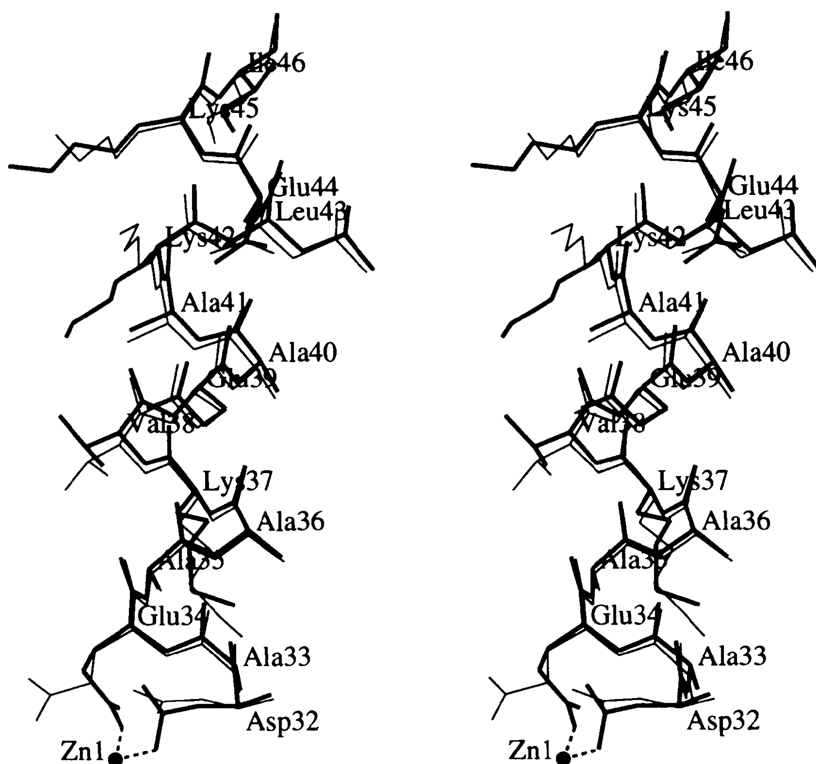

Fig. 7. The part of the RCCP-M110 molecule involved in dimer formation in comparison with the corresponding part of RCCP-SL. RCCP-M110 is drawn with thin lines, RCCP-SL is drawn with thick lines.

From these observations, we can conclude that the molecules in the dimer are not strongly associated in RCCP-SL and that dissociation in the crystal is most probably caused by Zn1 binding. The comparison of RCCP-M110 and RCCP-SL molecules (Fig. 7) indicates that the side chains of residues other than Glu34, the side chains of which are involved in molecule association in the dimer structure of RCCP-M110, also undergo conformational changes upon dimer dissociation or Zn-mediated interaction. In particular, changes in conformation of the side chains of Val38, Lys42 and Lys45 are apparent.

In conclusion, we have made two important observations: that transition metal ions can have profound effects on protein structure through alteration of molecule interactions, and that in RCCP, the dimer interaction is not very strong. Most cytochromes *c′* exist as dimers in solution and are difficult to dissociate because of the strong interaction between molecules. In some cases, ligand binding to the heme can lead to dimer dissociation, although not in RCCP. On the other hand, we have now shown that Zn binding at six different locations in RCCP can lead to dimer dissociation.

This work was supported in part by the Grant-in-Aid for Scientific Research on Priority Area (No. 05244102) to NY and a grant from the National Institutes of Health (GM21277) to MAC. THT was invited to the Himeji Institute of Technology by the Japanese Society for the Promotion of Science. This work has been accelerated by the High-Speed LAN Project promoted by BBCC. We are grateful to Richard Ambler for providing the unpublished amino-acid sequence of RCCP-SL.

References

Abola, F. C., Bernstein, F. C., Bryant, S. H., Koetzle, T. F. & Weng, J. (1987). *Crystallographic Databases – Information Content, Software Systems, Scientific Applications*, pp. 107–132. Bonn/Cambridge/Chester: IUCr.

Ambler, R. P., Bartsch, R. G., Daniel, M., Kamen, M. D., McLellan, L., Meyer, T. E. & Van Beeumen, J. (1981). *Proc. Natl Acad. Sci. USA*, **78**, 6854–6857.

Baker, E. N., Anderson, B. F., Dobbs, A. J. & Dodson, E. J. (1995). *Acta Cryst.* D**51**, 282–289.

Bartsch, R. G. (1978). *The Photosynthetic Bacteria*, edited by R. K. Clayton & W. Sistrom, pp. 249–280. New York: Plenum Press.

Bernstein, F. C., Koetzle, T. F., Williams, G. J. B., Meyer, E. F. Jr, Brice, M. D., Rodgers, J. R., Kennard, O., Shimanouchi, T. & Tasumi, M. (1977). *J. Mol. Biol.* **112**, 535–542.

Brünger, A. T. (1990*a*). *Acta Cryst.* A**46**, 46–57.

Brünger, A. T. (1990*b*). *X-PLOR Manual.* Version 2.1. Yale University, New Haven, USA.

Caffrey, M., Simorre, J.-P., Brutscher, B., Cusanovich, M. & Marion, D. (1995). *Biochemistry*, **34**, 5904–5912.

Cusanovich, M. A. (1971). *Biochim. Biophys. Acta*, **236**, 238–241.

Cusanovich, M. A., Meyer, T. E. & Tollin, G. (1987). *Adv. Bioinorg. Chem.* **7**, 37–91.

Doyle, M. L., Gill, S. J. & Cusanovich, M. A. (1986). *Biochemistry*, **25**, 2509–2516.
Engh, R. A. & Huber, R. (1991). *Acta Cryst.* A**47**, 392–400.
Finzel, B. C., Weber, P. C., Hardman, K. D. & Salemme, F. R. (1985). *J. Mol. Biol.* **186**, 627–643.
Higuchi, Y., Okama, Y., Kanda, T., Misaki, S., Yasuoka, N., Meyer, T. E. & Cusanovich, M. A. (1996). *Acta Cryst.* D**52**, 199–200.
Jancarik, J. & Kim, S.-H. (1991). *J. Appl. Cryst.* **24**, 409–411.
Kassner, R. J. (1991). *Biochim. Biophys. Acta*, **1058**, 8–12.
Matthews, B. W. (1968). *J. Mol. Biol.* **33**, 491–497.
Meyer, T. E. & Kamen, M. D. (1982). *Adv. Protein Chem.* **35**, 105–212.
Otwinowski, Z. (1986). *DENZO. An Oscillation Data Processing Program for Macromolecular Crystallography.* Yale University, Connecticut, USA.
Patel, M. J., Kassner, R. J., Meyer, T. E. & Cusanovich, M. A. (1989). *Biochemistry*, **28**, 2140–2144.
Ren, Z., Meyer, T. & McRee, D. E. (1993). *J. Mol. Biol.* **234**, 433–445.
Rubinov, S. C. & Kassner, R. J. (1984). *Biochemistry*, **23**, 2590–2595.
Sakabe, N. (1991). *Nucl. Instrum. Methods Phys. Res. A*, **303**, 448–463.
Tahirov, T. H., Meyer, T. E., Cusanovich, M. A., Misaki, S., Higuchi, Y. & Yasuoka, N. (1997). *J. Mol. Biol.* In the press.
Tahirov, T. H., Misaki, S., Meyer, T. E., Cusanovich, M. A., Higuchi, Y. & Yasuoka, N. (1996). *Nature Struct. Biol.* **3**, 1–6.
Weber, P. C., Bartsch, R. G., Cusanovich, M. A., Hamlin, R. C., Howard, A., Jordan, S. R., Kamen, M. D., Meyer, T. E., Weatherford, D. W., Xuong, N. H. & Salemme, F. R. (1980). *Nature (London)*, **286**, 302–304.
Weber, P. C., Howard, A., Xuong, N. H. & Salemme, F. R. (1981). *J. Mol. Biol.* **153**, 399–424.
Yasui, M., Harada, S., Kai, Y., Kasai, N., Kusunoki, M. & Matsuura, Y. (1992). *J. Biochem.* **111**, 317–324.